Articles in PresS. Am J Physiol Regul Integr Comp Physiol (August 11, 2010). doi:10.1152/ajpregu.00510.2009

Contractile Properties of Muscle Fibers from the Forelimb Deep and Superficial Digital Flexors of Horses

M.T. Butcher,[1,2] P.B. Chase,[2] J.W. Hermanson,[3] A.N. Clark,[2] N.M. Brunet,[4] and J.E.A. Bertram[5]

[1]Department of Biological Sciences, Youngstown State University, Youngstown, OH USA
[2]Department of Biological Science, Florida State University, Tallahassee, FL USA
[3]Department of Biomedical Sciences, College of Veterinary Medicine, Cornell University, Ithaca, NY USA
[4]Department of Biological Science, Program in Molecular Biophysics, Florida State University, Tallahassee, FL USA
[5]Department of Cell Biology and Anatomy, Faculty of Medicine, University of Calgary, Calgary AB Canada

Running title: Contractile properties of digital flexor muscle fibers

Word count: 6772 (intro-discussion)

2 Tables, 6 Figures

***Corresponding author full address:**

Michael Todd Butcher, Ph.D.
Department of Biological Sciences
4037 Ward Beecher Hall
Youngstown State University
Youngstown, OH 44555, USA
Email: (mtbutcher@ysu.edu)
Phone: 330-941-2195
Fax: 330-941-1483

Abstract

Equine digital flexor muscles have independent tendons but nearly identical mechanical relationship to the main joint they act upon. Yet these muscles have remarkable diversity in architecture, ranging from long, unipennate fibers ('short' compartment of DDF) to very short, multipennate fibers (SDF). To investigate the functional relevance of the form of the digital flexor muscles, fiber contractile properties were analyzed in the context of architecture differences and *in vivo* function during locomotion. Myosin heavy chain (MHC) isoform fiber type was studied and *in vitro* motility assays were used to measure actin filament sliding velocity (V_f). Skinned fiber contractile properties (isometric tension (P_0/CSA), velocity of unloaded shortening (V_{US}) and Force-Ca^{2+} relationships) at both 10°C and 30°C were characterized. Contractile properties were correlated with MHC isoform and their respective actin filament sliding velocities. The DDF contained a higher percentage of MHC-2A fibers with myosin (heavy meromyosin; HMM) and V_f that was 2-fold faster than SDF. At 30°C P_0/CSA was higher for DDF (103.5 ± 8.75 mN/mm^2) than SDF fibers (81.8 ± 7.71 mN/mm^2). Similarly, V_{US} (pCa 5, 30ºC) was faster for DDF (2.43 ± 0.53 FL s^{-1}) than SDF fibers (1.20 ± 0.22 FL s^{-1}). Active isometric tension increased with increasing Ca^{2+} concentration, with maximal Ca^{2+}-activation at pCa 5 at each temperature in fibers from each muscle. In general, the collective properties of DDF and SDF were consistent with fiber MHC isoform composition, muscle architecture and the respective functional roles of the two muscles in locomotion.

Keywords: Fiber, Horse, Muscle, Myosin, DDF, SDF

Introduction

The digital flexors of the equine forelimb provide a unique opportunity to investigate the integration of molecular composition, architectural organization and functional utilization of locomotor muscles in a large, cursorial mammal. Although their tendons have essentially equivalent relationships to the main joint they act upon, the metacarpo-phalangeal joint (fetlock) of the distal limb, they show remarkable diversity in their muscle architecture. The 'short' (humeral) compartment of the deep digital flexor (DDF) has long, unipennate fibers, while the superficial digital flexor (SDF) has short, multipennate fibers (**8, 20, 54**). Muscle architecture is an important component of musculoskeletal structure and function. For example, a short-fibered muscle with a long compliant tendon suggests a capacity for substantial elastic energy storage, an effective means to reduce metabolic cost in locomotion (**1**). Recent interest in understanding how architecture of the equine digital flexors relates to their function in the distal limb during locomotion has led to *in vivo* studies examining, first, isometric force production for characterization of the passive and active force properties of DDF and SDF muscles (**47**), and second, DDF and SDF contractile behavior and muscle-tendon unit function during walking and running (**9, 10**). General findings from these studies indicate that the functional roles of these two synergistic muscles differ, with the DDF (short) having a capacity to shorten to generate modest work and power during locomotion, while the SDF has extremely limited shortening capability, doing mostly negative work (i.e. eccentric contractions), with a capacity for high force production (high passive and active force) and large elastic energy storage in its tendon.

Amid these recent studies designed to better understand how such a diverse complex of muscles functions *in vivo*, basic physiological contractile properties of equine DDF and SDF muscle fibers remain largely unknown. Mechanical experiments on mammalian muscle fibers

have most often been performed on skinned (permeabilized) fibers from rabbits (**11-13, 35**) and even smaller mammals, such as rats and mice (**2, 3**), to determine fundamental measures of physiological capacity (e.g. maximum shortening velocity, V_0, or V_{US}). A thorough investigation of DDF and SDF contractile properties using single, skinned fibers would provide a valuable contribution toward understanding each muscle's functional capacity for contraction velocity, and thus work and power performance, as suggested by their respective architectures.

The velocity at which a muscle contracts (and performs mechanical work) is related to muscle fiber composition, which in turn, is mainly determined by the myosin heavy chain (MHC) isoforms expressed in the fibers (**35, 40**). Histochemical analyses have shown the DDF (short compartment) contains a higher percentage of fast fibers (Type II) while the SDF has relatively more slow fibers (Type I) (**20**). A high percentage of faster contracting fibers are common to work and power generating muscles whereas a high percentage of slow contracting fibers are found in postural muscles (i.e. muscles that produce force economically and maintain tension for extended periods), which are generally not considered important muscles in driving locomotion. Despite a thorough histochemical analysis of muscle fiber type, the MHC composition of DDF and SDF muscle fibers cannot be directly determined from these methods; gel electrophoresis allows identification of MHC isoforms at the single fiber level (**46, 52, 53**). When related to MHC composition, skinned fiber mechanics studies provide important links between muscle molecular composition, structure and function, and serve to clarify molecular bases of functional diversity among muscle fiber types (**5**).

In addition to fiber mechanics experiments, functional diversity present among the MHC isoforms can also be studied directly with *in vitro* motility assays using purified myosin (or the soluble heavy meromyosin (HMM) fragment) and fluorescently-labeled F-actin (**14, 19, 39**).

Motility assays on preparations of HMM from horse muscles have not previously been reported. Analysis of the MHC composition and measurements of filament sliding velocity (V_f) of myosin from DDF and SDF muscles will therefore be fundamental to characterization of the physiology and functional capacity of horse digital flexors.

The objective of this study was to characterize the physiological properties of DDF and SDF muscles and relate these properties to whole muscle architecture and function *in vivo*. Specific goals were to compare: 1. relative distribution of MHC isoforms expressed in fibers from DDF and SDF muscles to the underlying histochemical composition of the muscles, 2. function of myosin (i.e. HMM) from DDF and SDF muscles in motility assays at physiological temperature, and 3. DDF and SDF fiber contractile properties that are relevant to locomotion at a temperature near physiological. Based on the overall structure of these muscles and the existing histochemical analyses, it was hypothesized that the long-fibered DDF (short) has contractile properties relating to a faster MHC isoform composition while the short-fibered, multipennate SDF has properties more consistent with the slow (MHC-1) fiber type. This study will improve our understanding of the functional roles of the equine digital flexor muscles in locomotion and how cellular and molecular physiology contribute to this function.

METHODS

Ethical approval

All protocols for harvesting muscle tissue from horses were in accordance with the policies and standards of the Cornell University, College of Veterinary Medicine, Equine Hospital and IACUC approved guidelines and protocols. Rabbit muscle tissue for motility experiments was obtained according to protocols approved by the Florida State University IACUC.

Animals and muscle sampling

Five adult horses (two male Thoroughbreds, two female Thoroughbreds and one female Appaloosa) were used as muscle tissue donors for this study. The mean (± SD) age and body mass for the horses were 17.6 ± 4.8 years (range: 11-22 years) and 499.2 ± 42.9 kg (range: 454.5-545.4 kg), respectively. Horses used in this study were euthanized for reasons unrelated to this study but did not involve musculoskeletal lameness. Euthanasia was administered *via* barbiturate injection (Fatal-Plus, Vortech Pharmaceuticals Ltd., Dearborn, MI, USA) at the Cornell University, College of Veterinary Medicine, Equine Hospital. Following euthanasia, the DDF (humeral head, short compartment) and SDF muscles of the forelimb and the soleus (SOL) muscle (n = 2 horses) of the hindlimb were freshly removed and 2-3 fiber fascicles were dissected from the mid-belly region of each muscle and tied to Teflon® strips at *in vivo* length. Adjacent fascicles were sampled from superficial-to-deep regions of the muscles for fiber mechanics and fiber typing analyses.

Skinned fiber preparation

Freshly dissected muscle fibers from the DDF, SDF and SOL muscles were prepared for mechanical experimentation using published methods (**11, 12**). Fiber fascicles were treated with a skinning solution containing 0.5% Brij-58 detergent (Pierce Ultrapure; Pierce Biotechnology Inc., Rockford, IL USA) for 1 h on ice and then glycerinated with a 50% glycerol/skinning solution and stored at -20°C. Skinning solution contained (in mM): 25 EGTA, 50 MOPS, 6 Mg $(Acetate)_2$, 4 Acetic acid, 5 ATP, 0.03% (w/v) dithiothreitol (DTT) and 0.005% (w/v) Leupeptin (pH 7.1; 0-2°C). Single fibers (~2 mm segments) were isolated by microdissection in a cold bath (4°C) of 50% glycerol/relaxing solution. End compliance of the fibers was minimized by chemical fixation of the fiber ends using localized microapplication of 5% glutaraldehyde (plus 1 mg/ml fluorescein for visualization) (**11**). The fixed ends of the fibers (~0.5 mm) were

wrapped in aluminum foil T-clips (KEM-MIL Co., Hayward, CA USA) before being transferred to the experimental apparatus for attachment and mechanical measurements. A drop of silicone was added on each clip to stabilize placement on the hooks of the motor and force transducer.

Experimental Solutions

Relaxing and activating solutions were prepared as previously described (**11**). The basic composition of the solutions was (in mM): 5 MgATP, 1 Pi, 10 EGTA, 15 PCr (CP), 100 K^+ plus Na^+, 3 Mg^{2+}, 50 MOPS, 1 DTT, and 1 mg/ml creatine kinase (CK; 260 U ml^{-1}). Four stock solutions were made with the following [Ca^{2+}]'s: pCa 9 (relaxing solution), pCa 7, pCa 6 and pCa 5 (maximum activation), where pCa = $-Log_{10}[Ca^{2+}]$. [Ca^{2+}] in the stock solutions was adjusted by adding appropriate amounts of $Ca(acetate)_2$. Intermediate [Ca^{2+}] (pCa 6.4, pCa 6.2, pCa 5.9, pCa 5.8, pCa 5.6, pCa 5.4 and pCa 5.2) solutions were made from combinations of the stock solutions. The pH was adjusted to 7.0 for all stock solutions at 12ºC. Ionic strength was 0.18 M for all stock solutions and was adjusted with Tris and acetate. Experimental solutions were used at 10 and 30°C with no further adjustments to pH and ionic strength for minor changes with temperature as have been described (**4, 46**); solutions at pH 7.0 and physiological ionic strength of 0.18 M set at cooler temperatures have been shown to be adequate at higher temperatures (**51**). DTT and CK were added to relaxing and activating solutions on the day of each experiment.

Experimental apparatus for single, permeabilized fiber mechanics

The experimental apparatus for single, permeabilized fiber mechanics has been described in detail (**13, 25**). Relaxing and activating solutions were held in anodized aluminum wells (200 µl) on glass coverslips (no. 1 thickness). Wells were held in a wheel that could be rotated to immerse the fiber in any of twelve wells. The temperature of the wells was measured with a k-type thermocouple and was maintained at either 10°C or 30°C depending on the experiment.

Temperature for individual experiments was controlled within 1°C (model ATR-4 Adaptable Thermoregulator, Quest Scientific, North Vancouver, BC, Canada). Single fibers were attached via small hooks to a force transducer (2.2 kHz resonant frequency) (model 400A, Aurora Scientific Inc, Ontario, Canada) at one end and a servomotor (step time ≤ 300 μs; model 312C, Aurora Scientific Inc, Ontario, Canada) at the other. The force transducer and motor were mounted on the modified stage of an inverted microscope. Force and length signals were digitized using custom data acquisition software (NEWDAC; ref. **13**) on a PC-based system with a DT2831-G data acquisition board (Data Translation, Marlboro, MA USA). Stability of fiber structure and mechanical properties during activations were maintained as described by Brenner (**6**). Briefly, fibers were shortened transiently every 5 sec at a rate ≥ the maximum shortening velocity, which reduced force to zero. The periodic unloading of the fiber was followed by a quick re-stretch to isometric length (**11**). Fiber striation pattern was continuously monitored during experiments by a CCD camera (model XR-77, Sony Electronics Corp., Tokyo Japan).

Experimental protocol for single, permeabilized fiber mechanics

All mechanical measurements were made at both 10°C and 30°C. Isometric fiber length (L_0) and fiber diameter were measured in relaxing conditions using an optical micrometer in the eyepiece of the inverted microscope. L_0 was determined at 40x magnification as fiber length between end clips. Lengths of the two fixed ends were measured (in pCa 5) at the end of each experiment and subtracted from L_0 to obtain active fiber length (L_a). Fiber diameter was determined at 320x magnification as the average of three measurements at different locations along the fiber. Sarcomere length (L_s) was determined by HeNe laser diffraction (**12**). Initial L_s was set to 2.6 μm in relaxing conditions. Following a brief initial activation (10 s; pCa 5), fibers were returned to pCa 9, L_0 was adjusted to minimize passive tension, and L_s was re-measured.

Mean (± S.E.M.) L_s was 2.4 ± 0.03 μm (n = 32) for DDF fibers, 2.4 ± 0.03 μm (n = 32) for SDF fibers and 2.4 ± 0.07 μm (n = 16) for SOL fibers.

To determine isometric force (P), fibers were activated for about 30-60 s in sequentially higher [Ca^{2+}]'s in the following order: pCa 9, 7, 6.4, 6.2, 6, 5.9, 5.8, 5.6, 5.4, 5.2 and 5 (maximum isometric force, P = P_0, was determined at pCa 5). Measurements of P were made during the steady-state period before a Brenner cycle (**25**). P was normalized to fiber cross-sectional area (CSA) to give P/CSA (in mN mm^{-2}), where CSA was calculated from mean fiber diameter assuming circular geometry. To determine velocity of unloaded shortening (V_{US}), fibers were briefly relaxed following the series of force measurements before being transferred back to maximal activation conditions (pCa 5). Measurements of V_{US} were made using the slack-test method (**13, 17**). Briefly, a series of seven length steps were applied, each shortening the fiber by 0.035 to 0.12 L_0, beginning with the greatest length change. The resulting force changes were recorded for each length step. After completion of a length step, the fiber was held at the slack length until force began to re-develop. The time between completion of the length step and the point of force redevelopment is defined as slack time. Slack test data were digitized at sampling frequencies (256-3000 Hz) appropriate for optimal resolution.

Data analysis for single, permeabilized fiber mechanics

Force and length data records were analyzed using custom software (Fiber Analysis; ref. **13**). At each pCa, passive tension measured in relaxing conditions was subtracted from calculated P/CSA and values were averaged at each experimental temperature. Additionally, P/CSA at each pCa was also normalized to P_0/CSA at pCa 5 (for each fiber) for Force-Ca^{2+} relationship analysis. Normalized P/CSA values were plotted as a function of pCa for each fiber experiment and fit with a 2-parameter sigmoid Hill equation using nonlinear least squares regression (SigmaPlot 6.0, SPSS Inc., Chicago, IL USA). Slope (n) and pCa_{50} of the Force-Ca^{2+}

relationships were determined for DDF, SDF and SOL fibers for each experimental temperature from the Hill Plot regressions. V_{US} was calculated using both Fiber Analysis software to determine slack time and length change from force and length records, and a custom Slack Test analysis macro (linear least squares regression) written in MS Excel for Windows (Microsoft Systems Inc., Redmond, WA USA). V_{US} (in FL s^{-1}) was determined as the slope of the linear regression between length step size (normalized to L_a) and slack time. V_{US} for DDF, SDF and SOL fibers were averaged at each experimental temperature for maximally activated fibers (pCa 5). Values of P/CSA, Force-Ca^{2+} slope, pCa_{50} and V_{US} for SOL fibers served as a slow muscle control in these experiments.

Quality controls for high temperature

In skinned fibers, prolonged activation at higher temperatures can progressively disrupt stability of the fiber striation pattern and fiber function (**4, 39**). In addition to constant video monitoring, Brenner cycling was particularly important in maintaining fiber stability at 30°C. The similarity of force during first and last activations indicated that fiber structure and function remained stable throughout the protocol. Force at the end of experiments averaged 99% of that at the beginning for DDF fibers, 89% for SDF fibers and 100% for SOL fibers at 10°C. Average stability of force was 98% for DDF, 95% for SDF and again 100% for SOL fibers at 30°C.

Myosin isoform identification and fiber typing

Myosin heavy chain (MHC) isoform composition was analyzed for a separate set of DDF, SDF and SOL fibers adjacent to those used for contractility measurements. MHC isoforms of single fibers for each muscle were determined by SDS-PAGE using a combination of methods previously described (**46, 48**). Permeabilized fiber segments approximately 2 mm in length were denatured for 2 h at room temperature in 20 µl of Laemmli solution (**23**) with the following composition: 62.5 mM Tris, 2.3% (w/v) SDS, 10% glycerol and 5% (v/v) β-mercaptoethanol.

Denatured fiber samples were stored overnight at -20°C. Typically 5-10 µl of the denatured fiber sample was loaded onto the gels (mini slab gels). The acrylamide: *N, N'*–methylene-bisacrylamide ratio of the gels was 37.5:1, with total polyacrylamide percentage equaling 4% and 6% in the stacking and separating gels, respectively. Gel apparatus chambers (Mini-Gel System; Bio-Rad Laboratories, Hercules, CA USA) were filled with electrode buffer containing 25 mM Tris, 192 mM glycine and 0.1% SDS (pH 8.3) (**46**). Electrophoresis was run for 22-24 h at 100 V at 4°C (**48**). Gels were silver stained (Sigma ProteoSilver™ Stain Kit; Sigma Chemical Co., St. Louis, MO USA) for identification of protein bands.

MHC bands from single fibers were evaluated by comparing band migration to both molecular weight standards in the 200 kDa region and MHC from bulk myosin samples purified from entire muscle fascicles. Briefly, myosin was extracted from the remaining skinned fascicles by homogenizing ~30 mg of muscle on ice in 1 ml of a high salt buffer containing (in mM): 250 sucrose, 300 KCl, 5 EDTA and 10 Tris. Precipitated myosin was then centrifuged for 10 min, the pellet was collected, solubilized in Laemmli solution for 1 h at room temperature, and stored overnight at -20°C. Typically, 3-5 µl of purified myosin samples were loaded in the end lanes of gels and used as references for identifying MHC isoforms present in DDF, SDF and SOL fibers. Percentages of each MHC isoform were quantified from the total number of fibers sampled from each muscle and each horse. Percent distribution of MHC isoforms for the overall number of fibers sampled from each muscle (i.e. population) was also quantified.

Fiber type staining (histo/immunohistochemistry) was performed using established methods (**20**). Briefly, histochemical staining followed protocols for myosin ATPase originally derived from Brooke and Kaiser (**7**) and Padykula and Herman (**29**). Slow and fast properties of fibers were estimated by myosin ATPase staining of continuous serial tissue sections. For

immunohistochemistry, serial sections were first reacted with one of several primary, MHC isoform-specific antibodies for 16-18 hrs at 4°C, followed by reaction against secondary antibody (anti-mouse) and DAB staining with a Zymed Histostain Plus kit (Zymed Laboratories, San Francisco, CA). Primary antibodies were S58 (provided by Dr. Frank Stockdale, Stanford Medical School), which reacts with vertebrate slow myosin (MHC-1), and MY32 (Sigma Chemical Co., St. Louis, MO USA), which reacts against vertebrate fast myosins. Additionally, the SC71 antibody (ATTC, Raleigh, NC USA), which has yielded positive reaction against the fast MHC-2A isoform, was used.

Myosin preparation and *in vitro* motility assay

Myosin from DDF (humeral head, short compartment) and SDF muscles from a Thoroughbred horse, and myosin from the psoas muscle and F-actin from the back and leg muscles of New Zealand White rabbits were prepared according to established methods (**24, 30**). Chymotryptic digestion of myosin from each muscle was used to obtain the soluble heavy meromyosin fragment (HMM) and samples were stored at 4°C. In addition, F-actin was fluorescently labeled with rhodamine-phalloidin (RhPh) (**19, 22**). On the day of the experiments, ATP-insensitive myosin heads were removed from HMM by ultracentrifugation in the presence of unlabelled F-actin and MgATP (**22**) followed by adjustment of the HMM concentration (range: 0.20-0.35 mg/ml) for each muscle's HMM sample. Motility experiments took place within 1-2 days after HMM purification using an assay protocol derived with slight modification from that previously described (**14**).

Motility assays were carried out in flow cells constructed of a glass coverslip coated with a thin layer of 0.1% nitrocellulose in amyl acetate mounted on an untreated microscope slide using spacers cut from no. 1.5 glass coverslips and silicone high-vacuum grease applied by syringe. Motility solutions were applied at room temperature in a standardized order (**14**). Briefly, an

HMM sample was adsorbed (two applications 1 min apart) onto the coated inner flow cell surface. Next, 0.5 mg/ml bovine serum albumin (BSA) in actin buffer (AB, in mM: 25 KCl, 25 imidazole, 4 $MgCl_2$, 1 EGTA, 1 DTT, pH 7.4) was applied for 1 min to block non-specific protein binding followed by an AB wash to remove unbound BSA. Sheared and unlabeled F-actin was then applied for 1 min to inhibit binding of RhPh labeled F-actin to any remaining ATP-insensitive heads. Next, 0.5 mM ATP in AB was applied to dissociate the unlabeled F-actin from active myosin heads, followed by an AB wash. Then, fluorescently labeled F-actin (~8 nM actin monomer) was applied and allowed to bind to HMM; after 1 min, unbound filaments were removed with an AB wash. Finally, an aliquot of motility buffer (MB) was applied to flow cells to initiate RhPh F-actin motility. Motility buffer consisted of AB plus 2 mM ATP; 16.7 mM glucose, 100 μg/ml glucose oxidase, 18 μg/ml catalase and an extra 40 mM DTT were added to minimize photo-bleaching of fluorescently labeled F-actin and limit photo-oxidative damage to the proteins (**22**).

After addition of MB, flow cells were transferred to the stage of a Diastar upright fluorescence microscope (Leica, Deerfield, IL USA) and 1 min was allowed for temperature equilibration (**19**). Flow cell temperature was maintained at either 28°C (standard temperature) or 38°C (physiological core body temperature for a horse) by circulating temperature-controlled water through a copper coil surrounding the microscope objective; temperature was calibrated within flow cells, directly under the objective. Image capture of F-actin motility was accomplished with a silicon intensifier target camera (model VE 1000; Dage-MTI, Michigan City, IN USA) at 30 frames s^{-1}, with an added time-date generator signal (model WJ-810; Panasonic, Secaucus, NJ USA) and stored on VHS videocassettes (VCR model AG7350; Panasonic) for analysis as described (**14**). A count of 6-10 trial image recordings of 30-60 s

duration each were made per flow cell. Three flow cells were sampled for each type of HMM (DDF, SDF, rabbit psoas) at each temperature for a total sample size of n = 18 flow cells.

Data analysis for *in vitro* motility assays

Recorded images of RhPh labeled F-actin motility were digitized and analysis of filament sliding speed (V_f) was carried out with the aid of MetaMorph® software (Universal Imaging, Molecular Devices Corp., Downingtown, PA USA) as previously described (**28**). For each flow cell, 12 stacks of frames were created from the digitized recordings; each stack consisted of 30 frames (1 s of recorded data) or 90 frames (3 s of recorded data) of motility data. Individual actin filament paths were then visualized by creating a superimposed image of all frames of one stack, called a projection, and subtracting the image of the first frame from that projection. For each stack, 5 filaments were randomly selected and the distance travelled (d) was estimated by manually measuring the residual contour lines of their respective pathways. Finally, V_f (in $\mu m\ s^{-1}$) was determined as $d/(t(\#frames-1))$, where t is the frame-to-frame duration, i.e., $(frame\ rate)^{-1}$. Individual filament measurements of V_f for DDF, SDF or rabbit psoas HMM were averaged (n = 180 filaments per muscle) for each experimental temperature and their distribution characterized by non-parametric statistics due to the large differences among means of V_f and corresponding low error terms. V_f of rabbit psoas HMM, with a near 100% composition of the MHC-2X isoform (**40**), served as a fast myosin (control) in these experiments.

Statistical analysis

All data are expressed as means ± SE. Statistical significance of the differences among means of P_o/CSA, V_{US}, Force-Ca^{2+} relationship slope and pCa_{50} of fibers for each muscle and experimental temperature (10°C and 30°C) were assessed by 2-way analysis of variance (ANOVA) followed by a Holm-Sidak multiple comparison test. Considering V_f data were not found to be normally distributed and failed to meet the assumption of equal variances, statistical

significance of the differences among means of V_f for each muscle's HMM and experimental temperature (28°C and 38°C) was assessed by an ANOVA for Ranks followed by a Dunn's multiple comparison test. Particular emphasis of both fiber mechanics and motility V_f analyses was placed on differences between means of DDF and SDF preparations. Statistical significance for all tests was accepted at $p \leq 0.05$.

RESULTS

MHC isoform composition

Myosin ATPase and antibody staining on large cross-sections of DDF (see Fig. 1) and SDF muscle fibers showed distributions of slow (MHC-1) and fast (MHC-2A) fibers from the population sampled (n = 1000 fibers/muscle) in this analysis were 29% and 71%, respectively, for DDF, and 60% and 40% for SDF. Electrophoretic (SDS-PAGE) results of single fibers showed good consistency with fiber type staining analyses. For each muscle sampled, protein bands from only two MHC isoforms were clearly identified, MHC-1 and MHC-2A (see Fig. 2). Slow MHC-1 migrated faster than MHC-2A and generally migrated to the same position for DDF, SDF and SOL muscle samples from horse. SDS-PAGE identification of MHC isoforms in single permeabilized fibers from DDF, SDF and SOL is illustrated in Fig. 2 and summary statistics from this separate analysis of individual fibers are presented in Table 1. The typically slow SOL muscle contained 100% MHC-1 fibers. Distributions for MHC-1 and MHC-2A isoforms from the population of fibers sampled were 12.7% and 83.5%, respectively, for DDF (n = 79 fibers), and 44.3% and 48.1% for SDF (n = 79 fibers). A small percentage of hybrid MHC-1-2A fibers were also identified in DDF (3.8%) and SDF (7.6%).

Filament sliding velocity (V_f)

Fig. 3 illustrates the large disparity among means of V_f from motility assays with HMM prepared from bulk muscle samples of horse DDF or SDF myosin, or rabbit psoas myosin.

Means of V_f were significantly different ($p<0.001$) among the three muscles for each experimental temperature (28ºC or 38ºC). As expected for each muscle, V_f at 38ºC was faster than at 28ºC. Compared with rabbit psoas myosin (fast control), means of V_f for DDF and SDF were 3.7-8.3x lower at 28°C, and 2.3-5.4x lower at 38°C. Mean V_f for SDF myosin was consistently about 2.3x lower than for DDF myosin regardless of experimental temperature.

Fiber Contractile Properties

Maximum isometric tension (P_0/CSA)

Fig. 4 illustrates the force response of a single fiber to sequentially increasing [Ca^{2+}] over the time course of an entire experimental protocol at 30ºC; parameters for maximum Ca^{2+}-activation (P_0/CSA and V_{US}) were obtained during the latter part of the protocol (pCa 5). Frequency distributions of P_0/CSA for DDF, SDF and SOL fibers at 30°C are shown in Fig. 5A. Means (± SE) of P_0/CSA at both 10ºC and 30ºC are presented in Table 2. Mean P_0/CSA of DDF fibers was just significantly different ($p = 0.03$-0.05) compared with SDF or SOL fibers at either temperature, although the large difference between mean P_0/CSA for SOL fibers (46.7 ± 4.5 mN mm^{-2}) and DDF fibers (93.3 ± 7.3 mN mm^{-2}) at 10°C was highly significant ($p<0.0001$). Means of P_0/CSA were also found to be just significantly different between SOL and SDF fibers ($p = 0.04$) at 10°C, although the values at 30ºC for SOL fibers and SDF fibers were similar ($p = 0.77$) due primarily to the significant increase in slow SOL fiber P_0/CSA with temperature.

Velocity of unloaded shortening (V_{US})

Fig. 5B shows frequency distributions of V_{US} for DDF, SDF and SOL fibers at 30°C. Means (± SE) of V_{US} determined at maximal activation (pCa 5) are presented in Table 2. Mean V_{US} of DDF fibers was not significantly different compared with mean V_{US} for both SDF and SOL fibers at 30°C; this may be due to the apparently bimodal distribution of V_{US} values from DDF (Fig. 5B), as could be expected from the mixture of fiber types found by histochemical and SDS-

PAGE analyses (Figs. 1, 2; Table 1). Differences in mean V_{US} at 10°C, however, were statistically significant between SOL and DDF fibers ($p = 0.006$). As expected, mean V_{US} increased significantly with temperature for DDF, SDF and SOL fibers. This increase, in large part, accounted for the similarity ($p = 0.89$) between V_{US} for SOL fibers (1.07 ± 0.21 FL s^{-1}) and V_{US} for SDF fibers (1.2 ± 0.22 FL s^{-1}) at 30°C even though the distribution of V_{US} values was broader for SDF than for SOL fibers (Fig. 5B).

Force-Ca^{2+} relationship parameters

Fig. 6 shows averaged Force-Ca^{2+} relationships for DDF, SDF and SOL fibers at both experimental temperatures. The slopes of these relationships for DDF and SDF fibers appear similar at 10ºC and 30ºC but both appear different from SOL. Statistical comparisons of the curve parameters determined for individual fiber experiments revealed that the mean slopes (*n*) of the Force-Ca^{2+} relationships were significantly different between SOL and DDF fibers (1.63 ± 0.12 *vs.* 3.00 ± 0.22; $p = 0.002$) and SOL and SDF fibers (1.63 ± 0.12 *vs.* 2.54 ± 0.31; $p = 0.045$) at 10°C, while neither DDF nor SDF slopes differed from that of SOL fibers at 30°C. The slopes of the DDF and SDF fibers were also not significantly different at either temperature. Mean slopes for each muscle did not vary significantly with temperature (e.g. a slope of 2.5 for SDF fibers was determined for both 10°C and 30°C).

Hill regression analysis used to determine Force-Ca^{2+} relationships for individual fibers from each muscle provided measurements of the pCa_{50} for each relationship. Like Force-Ca^{2+} relationship slope, mean pCa_{50} for SOL fibers was significantly different from DDF fibers (6.18 ± 0.03 *vs*. 6.01 ± 0.03; $p = 0.01$) and SDF fibers (6.18 ± 0.03 *vs*. 6.05 ± 0.05; $p = 0.04$) at 10°C. Significant differences between mean pCa_{50} of SOL fibers and DDF (6.23 ± 0.05 *vs*. 6.08 ± 0.06; $p = 0.03$) or SDF (6.23 ± 0.05 *vs*. 6.00 ± 0.05; $p = 0.001$) fibers, were also found at 30ºC, whereas mean pCa_{50} was not statistically significant between DDF and SDF fibers for either

temperature (Fig. 6). Within each muscle, mean values of pCa_{50} again did not vary significantly with temperature, ranging from pCa 6.0-6.2 for all three muscles.

DISCUSSION

The main objective of this study was to characterize and compare cellular and molecular contractile properties between equine DDF and SDF muscles and relate these properties to their muscle architecture and function *in vivo*. These muscles have similar apparent action around the metacarpophalangeal joint, but substantially different architecture. Motility and fiber mechanical studies were conducted at two experimental temperatures so that comparisons could be made with past studies (typically at sub-physiological temperatures) and to establish functional parameters at temperatures that more closely approximate physiological function.

MHC Isoform Composition

Large mammals typically express three conventional MHC isoforms (MHC-1, MHC-2A, MHC-2X) in their skeletal muscles (**15**). For example, the equine gluteus medius, a powerful hindlimb muscle for locomotor propulsion, has been shown to contain a relatively high percentage of fast MHC-2X fibers in addition to MHC-2A and MHC-1 fibers (**36, 42**). Other, more specialized muscles of the distal hindlimb or forelimb, however, do not show concurrent expression of all three isoform fiber types (soleus: **21, 27**; interosseus: **43**), and may be expected to have a primary composition of MHC-1 and MHC-2A fibers as evidenced in the forelimb digital flexor muscles of horses in this study.

Fiber typing results for DDF and SDF by electrophoresis (Table 1; Fig. 2) and histo/immunohistochemical techniques (Fig. 1) compare well with available fiber type data for these two muscles. Inferring MHC isoform, the DDF (short) was reported to contain 44% MHC-1 and 51% MHC-2A fibers, while the SDF contained 59% MHC-1 and 39% MHC-2A fibers (**20**). The same study also indicated each muscle contained a small percentage of MHC-2X fibers

(reported as Type IIB, consistent with classification at that time). A recent immunohistochemical study of fiber types in Thoroughbred horses specifies a composition of 76% MHC-2A fibers in the DDF (head of this complex muscle not noted), 57% MHC-2A fibers in the SDF, and 0% MHC-2X fibers in both muscles (**21**). Despite slight differences in the calculated percentages of each fiber type among the previous and the present study, all confirm a primary composition of MHC-1 and MHC-2A isoforms in the DDF and SDF muscles. The very small percentage of fibers previously inferred to be MHC-2X in DDF short compartment (**20**) and the lack of MHC-2X fibers identified in this study and in a recently published report (**21**), suggest the MHC-2X isoform may not significantly contribute to contractile function of the forelimb DDF and SDF muscles during locomotion. Furthermore, age, breed and training effects may be factors that influence fiber type distributions observed in horses (**21, 37**). Although assessment of these factors is beyond the scope of this study, we speculate that the consistent composition of MHC-1 and MHC-2A fibers in the specialized digital flexor muscles may be a feature fundamental to *equus* given the broad ranges of age, breed and training level of horses used in studies (**20, 21**) for which percentage fiber type has been determined.

Myosin Functional Capacity and Fiber Contractile Properties

MHC isoform composition in muscle fibers is the primary determinant of skeletal muscle contractile properties and performance (**5, 40**). At the molecular level (purified HMM), V_f at body temperature of the horse (38ºC) provides realistic estimates of physiological myosin function (i.e. contractile velocity) in the digital flexor muscles. V_f for DDF was significantly faster (2x) than V_f for SDF at 38°C (Fig. 3). These motility data indicate a good correlation between MHC isoform composition of a muscle and functional properties of its constituent myosin molecules. The large mean difference likely reflects functional heterogeneity in MHC isoforms between the DDF and SDF muscles. MHC-2A isoforms hydrolyze ATP at faster rates

than MHC-1 isoforms and thus actin filament interactions (i.e. cross-bridge cycling) occur at faster rates. Slower detaching myosin heads of MHC-1 isoforms in a heterogeneous HMM sample create internal drag forces and slow V_f by counteracting the faster acto-myosin cycling rates of MHC-2A isoforms (**18**). Therefore, the DDF with a comparatively higher percentage of the MHC-2A isoform has a higher mean V_f and thus potential for faster contractile properties at the fiber level, consistent with our main hypothesis.

DDF and SDF fibers showed similar Ca^{2+}-dependence of steady-state isometric force (Fig. 6) while DDF fibers developed higher isometric tension than SDF fibers and on average, shortened twice as fast at 30ºC (Table 2). Overall, these findings may be explained by the heterogeneous composition of MHC-1 and MHC-2A fibers in both muscles, with the DDF having a higher percentage of fast MHC-2A fibers. However, while our study does not allow us to rule out the possibility that observed differences in contractile properties between DDF and SDF resulted from intrinsically different properties of the same fiber type, previous studies of skinned fibers (**5, 32, 49, 50**) indicate that contractile properties at saturating Ca^{2+} generally correlate with MHC isoform, while thin filament proteins troponin and tropomyosin are also important for properties at sub-saturating Ca^{2+} levels. Despite the evaluation of differences in contractile properties being limited to a set of mean measurements between two muscles instead of a specific fiber type, comparisons between the mixed fiber type DDF and SDF muscles are consistent with the main objective of this study. Furthermore, we should not expect to find differences in properties of the same fiber type sampled from different muscles and compared within a species.

Contractile property data available for muscle fibers of large mammals indicate properties of homologous MHC isoform fiber types (i.e. within a species, different muscles) are generally

similar (**32, 49, 50**). Accord between DDF and SDF fiber properties reported in this study and previously published data bolsters confidence in validity and, where applicable, repeatability of these parameters for the horse. Mean P_0/CSA for DDF and SDF fibers at 10ºC are well within the range of isometric tension values of 84 mN mm^{-2} and 97 mN mm^{-2} (15ºC) reported for horse muscle fibers (**38**) identified as MHC-1 and MHC-2A respectively, by SDS-PAGE analysis of MLC (myosin light chains; ref. **44**). A mean V_{US} of 0.33 FL s^{-1} (15ºC) for MHC-1 fibers from the same study (**38**), is identical to the mean V_{US} of slow SOL fibers at 10ºC in this study. The similarity of contractile properties of a known fiber type between species (i.e. orthologous MHC isoforms) of similar size is equally remarkable. Means of P_0/CSA and V_{US} for DDF, SDF, and SOL fibers at 10°C (Table 2) are in good agreement with comparable data measured for MHC-1 and MHC-2A fibers from skeletal muscles in 400-500 kg cows (**51**). In the case of V_{US}, consistent observations for a known fiber type between cows and horses likely reflect the strong dependence of V_{US} on body size (**32, 38, 41, 49, 50, 53**). While the consistency among fiber contractile property data from similarly-sized mammals (and measured under similar conditions) is notable, more studies are needed for confirmation of these observations.

Relatively few studies have investigated contractile properties of skinned muscle fibers near physiological temperatures (**31, 34, 45, 46, 55**). Data reported herein are the first measured contractile properties of muscle fibers from a large mammal at higher temperature. Overall P_0/CSA increased moderately with temperature for DDF and SDF (ratio of P_0/CSA at 30°C:10°C = 1.11 DDF; = 1.12 SDF). Changes in isometric tension with temperature are consistent with those observed in other studies of skinned fibers, although means of P_0/CSA at 30ºC for DDF and SDF fibers are relatively lower. Differences in temperature dependence of isometric tension for horse muscle fibers compared with rabbit (**31, 34)** and human (**4, 46**) fibers may be related to

variation in temperature sensitivity depending on either the temperature range studied or species studied. The modest increase in P_0/CSA in DDF and SDF muscles may also be attributed to reduced temperature sensitivity of isometric tension in faster contracting fiber types at temperature of 30°C and above (**33, 34, 45, 46, 51**). This is reasonable given the marked presence of the fast MHC-2A isoform in both DDF and SDF fibers, and the higher temperature sensitivity of MHC-1 fibers (ratio of P_0/CSA at 30°C:10°C = 1.67 SOL). Comparison of V_{US} between DDF and SDF fibers at 30ºC is also indicative of the influence of a composition of MHC-1 and MHC-2A isoforms. The apparent bimodal distribution of V_{US} values for individual DDF fibers is suggestive of a higher percentage of fast MHC-2A fibers in this muscle (Fig. 5B). Although differences in mean V_{US} were not statistically significant between the DDF and SDF, V_{US} measurements have been shown to be more variable at higher experimental temperatures (**4**) and MHC-1 fibers demonstrate a greater temperature sensitivity of shortening velocity (**33**), which may have disproportionately increased V_{US} of slow contracting fibers.

Architecture and Physiology of the Digital Flexor Muscle Fibers in Horse Locomotion

In the distal forelimb of the horse, the DDF and SDF muscles share a similar mechanical advantage about the metacarpophalangeal joint (fetlock), however, muscle architecture of each muscle-tendon unit differs greatly, as do their functional roles in locomotion. The comparatively fast contracting DDF muscle (short compartment, humeral head) with its long fibers in a unipennate arrangement (**20, 54**), shortens to generate modest amounts of mechanical work during locomotion, thus contributing to flexion of the digit late in the swing phase (**9, 10**). *In vivo* performance of the DDF is consistent with a muscle composed of long and predominately fast MHC-2A isoform fibers. In particular, fast isoform fibers have intrinsically faster rates of cross-bridge cycling and the capacity to shorten at velocities several times faster than slow contracting fibers (**38, 49, 50**) where mechanical power generation is greater (**5**).

In contrast to the DDF, during locomotion, the short, multipennate fibers of the SDF (**8, 20, 54)** undergo isometric and lengthening (eccentric) contraction, allowing the muscle to produce high force economically and its tendon to store large amounts of elastic strain energy (**9, 10**). A muscle that has a role of high force production by little-to-no change in length of its fibers, is less dependent on fast MHC isoforms and fast shortening velocities of the muscle fibers for peak *in vivo* performance. Compared with the DDF, a higher percentage of slow MHC-1 fibers and slower contractile properties, are also considered to be consistent with the functional role of the SDF muscle in locomotion. Despite the capacity to shorten faster than slow isoform fibers, mammalian fast MHC-2A fibers have higher oxidative capacity (i.e. mitochondrial content) than MHC-1 fibers (**16, 26**). Therefore in the context of force producing muscle as opposed to a power generating muscle, both MHC-1 and MHC-2A fibers arranged in a multipennate architecture can provide high force capacity by isometric or eccentric contractions with the benefit of consuming less metabolic energy.

Perspectives and Significance

The diverse *in vivo* contractile behaviors of the DDF and SDF muscles match well with each muscle's architecture and physiological properties, with direct consequences for the energetic cost of locomotion in horses. A primary composition of MHC-1 and MHC-2A isoform fibers alone, arguably, reflects an evolutionary specialization for metabolic energy savings, although it appears that fiber architecture may be more influential in determining the functional role of each muscle in locomotion. The relative distributions of slow and fast MHC isoforms and the lack of substantial differences in fiber contractile properties between DDF and SDF further suggest that architecture of specialized distal limb muscles may be an evolutionary constraint on contractile physiology, and function. The distal limbs of cursorial animals display numerous morphological specializations for economical running that are perhaps best exemplified by the equine SDF (and

interosseous), an oxidative muscle with extremely short fibers arranged in a multipennate architecture. Muscles like the SDF are much less suited for mechanical work and power generation, but rather are highly specialized for economical, high force production. Distinctions in physiology and function displayed in equine digital flexors may therefore represent features of limb morphology that are fundamental to the evolution of all economical, long distance running animals.

REFERENCES

1. **Biewener AA**. Muscle-tendon stresses and elastic energy storage during locomotion in the horse. *Comp Biochem Physiol B* 120: 73-87, 1998.

2. **Bottinelli R, Schiaffino S, Reggiani C.** Force-velocity relations and myosin heavy chain isoform compositions of skinned fibers from rat skeletal muscle. *J Physiol* 437: 655-672, 1991.

3. **Bottinelli R, Canepari M, Reggiani C, Stienen GJ.** Myofibrillar ATPase activity during isometric contraction and isomyosin composition in rat single skinned muscle fibers. *J Physiol* 481: 663-675, 1994.

4. **Bottinelli R, Canepari M, Pellegrino MA, Reggiani C.** Force-velocity properties of human skeletal muscle fibers: myosin heavy chain isoform and temperature dependence. *J Physiol* 495: 573-586, 1996.

5. **Bottinelli R, Pellegrino MA, Canepari M, Rossi R, Reggiani C.** Specific contributions of various muscle fiber types to human muscle performance: an *in vitro* study. *J Electromyo Kinesiol* 9: 87-95, 1999.

6. **Brenner B.** Technique for stabilizing the striation pattern in maximally calcium-activated skinned rabbit psoas fibers. *Biophys J* 41: 99-102, 1983.

7. **Brooke MH, Kaiser KK.** Three "myosin adenosine triphosphatase" systems: the nature of their sulfhydryl dependence. *J Histochem Cytochem* 18: 670-672, 1970.

8. **Brown NAT, Kawcak CE, Mcllwraith W, Pandy MG.** Architectural properties of distal forelimb muscles in horses, *Equus caballus*. *J Morphol* 258: 106-114, 2003.

9. **Butcher MT, Hermanson JW, Ducharme NG, Mitchell LM, Soderholm LV, Bertram JEA.** Superficial digital flexor tendon lesions in racehorses as a sequelae to muscle fatigue. *Equine vet J* 39: 540-545, 2007.

10. **Butcher MT, Hermanson JW, Ducharme NG, Mitchell LM, Soderholm LV, Bertram JEA.** Contractile behavior of the forelimb digital flexors during steady-state locomotion in horses (*Equus caballus*): an initial test of muscle architectural hypotheses about *in vivo* function. *Comp Biochem Physiol A* 152: 100-114, 2009.

11. **Chase PB, Kushmerick MJ.** Effects of pH on contraction of rabbit fast and slow skeletal muscle fibers. *Biophys J* 53: 935-946, 1988.

12. **Chase PB, Martyn DA, Hannon JD.** Isometric force redevelopment of skinned muscle fibers from rabbit activated with and without Ca^{2+}. *Biophys J* 67: 1994-2001, 1994.

13. **Chase PB, Denkinger TM, Kushmerick MJ.** Effect of viscosity on mechanics of single, skinned fibers from rabbit psoas muscle. *Biophys J* 74: 1428-1438, 1998.

14. **Chase PB, Chen Y, Kulin KL, Daniel TL.** Viscosity and solute dependence of F-actin translocation by rabbit skeletal heavy meromyosin. *Am J Physiol Cell Physiol* 278: C1088-1098, 2000.

15. **Chikuni K, Muroya S, Nakajima I.** Absence of the functional myosin heavy chain 2b isoform in equine skeletal muscles. *Zool Sci* 21: 589-596, 2004.

16. **Delp MD, Duan C.** Composition and size of type I, IIA, IID/X, and IIB fibers and citrate synthase activity of rat muscle. *J Appl Physiol* 80: 261-70, 1996.

17. **Edman KAP.** The velocity of unloaded shortening and its relation to sarcomere length and isometric force in vertebrate muscle fibers. *J Physiol* 291: 143-159, 1979.

18. **Fitts RH, Bodine SC, Romatowski JG, Widrick JJ.** Velocity, force, power and Ca^{2+} sensitivity of fast and slow monkey skeletal muscle fibers. *J Appl Physiol* 84: 1776-1787, 1998.

19. **Gordon AM, LaMadrid MA, Chen Y, Luo Z, Chase PB.** Calcium regulation of skeletal muscle thin filament motility *in vitro*. *Biophys J* 72: 1295-307, 1997.

20. **Hermanson JW, Cobb MA.** Four forearm flexor muscles of the horse*, Equus caballus*: anatomy and histochemistry. *J Morphol* 212: 269-280, 1992.

21. **Kawai M, Minami Y, Sayama Y, Kuwano A, Hiraga A, Miyata H.** Muscle fiber population and biochemical properties of whole body muscles in Thoroughbred horses. *Anat Rec* 292: 1663-1669, 2009.

22. **Kron SJ, Toyoshima YY, Uyeda TQP, Spudich JA**. Assays for actin sliding movement over myosin-coated surfaces. *Methods Enzymol* 196: 399-416, 1991.

23. **Laemmli UK.** Cleavage of structural proteins during the assembly of the head of bacteriophage T4. *Nature* 227: 680-685, 1970.

24. **Margossian SS, Lowey S.** Preparation of myosin and its subfragments from rabbit skeletal muscle. *Methods Enzymol* 85: 55-71, 1982.

25. **Martyn DA, Chase PB, Hannon JD, Huntsman LL, Kushmerick MJ, Gordon AM.** Unloaded shortening of skinned muscle fibers from rabbit activated with and without Ca^{2+}. *Biophys J* 67: 1984-1993, 1994.

26. **Mattsona JP, Millerb TA, Poolec DC, Delp MD.** Fiber composition and oxidative capacity of hamster skeletal muscle. *J Histochem Cytochem* 50:1685–1692, 2002.

27. **Meyers RA, Hermanson JW.** Horse soleus muscle: postural sensor or vestigial structure? *Anat Rec A Discov Mol Cell Evol Biol* 288: 1068-1076, 2006.

28. **Mihajlović G, Brunet NM, Trbović P, Xiong P, von Molnár S, Chase PB.** All-electrical switching and control mechanism for actomyosin-powered nanoactuators. *Appl Phys Lett* 85: 1060-1062, 2004.

29. **Padykula HA, Herman E.** The specificity of the histochemical methods of adenosine triphosphatase. *J Histochem Cytochem* 3: 170-195, 1955.

30. **Pardee JD, Spudich JA.** Purification of muscle actin. *Methods Enzymol* 85: 164-181, 1982.

31. **Pate E, Wilson GJ, Bhimani M, Cooke R**. Temperature dependence of the inhibitory effects of orthovanadate on shortening velocity in fast skeletal muscle. *Biophys J* 66: 1554-1652, 1994.

32. **Pellegrino MA, Canepari M, Rossi R, D'Antona G, Reggiani C, Bottinelli R.** Orthologous myosin isoforms and scaling of shortening velocity with body size in mouse, rat, rabbit and human muscles. *J Physiol* **546,** 677-689, 2003.

33. **Ranatunga KW**. The force-velocity relation of fast- and slow-twitch muscles examined at different temperatures. *J Physiol* 351: 517-529, 1984.

34. **Ranatunga KW**. Endothermic force generation in fast and slow mammalian (rabbit) muscle fibers. *Biophys J* 71: 1905-1913, 1996.

35. **Reiser PJ, Moss RL, Giulian GG, Greaser ML.** Shortening velocity in single fibers from adult rabbit soleus muscles is correlated with myosin heavy chain composition. *J Biol Chem* 260: 9077-9080, 1985.

36. **Rivero JL, Serrano AL, Barrey E, Vallete JP, Jouglin M.** Analysis of myosin heavy chains at the protein level in horse skeletal muscle. *J Muscle Res Cell Motil* 20: 211-221**,** 1999.

37. **Rivero JL, Ruz A, Marti-Korff S, Estepa JC, Aquilera-Tejero E, Werkman J, Sobotta M, Lindner A.** Effects of intensity and duration of exercise on muscular responses to training of Thoroughbred racehorses. *J Appl Phsiol* 102: 1871-1882, 2007.

38. **Rome LC, Sosnicki AA, Goble DO**. Maximum velocity of shortening of three fiber types from horse soleus muscle: implications for scaling with body size. *J Physiol* 431: 173-185, 1990.

39. **Rossi R, Maffei M, Bottinelli R, Canepari M.** Temperature dependence of speed of actin filaments propelled by slow and fast skeletal myosin isoforms. *J Appl Physiol* 99: 2239-2245, 2005.

40. **Schiaffino S, Reggiani C.** Molecular diversity of myofibrillar proteins: gene regulation and functional significance. *Physiol Rev* 76: 371-423, 1996.

41. **Seow CY, Ford LE.** Shortening velocity and power output of skinned muscle fibers from mammals having a 25,000-fold range of body mass. *J Gen Physiol* 97: 541-560, 1991.

42. **Serrano AL, Petrie JL, Rivero JL, Hermanson JW.** Myosin isoforms and muscle fiber characteristics in equine gluteus medius muscle. *Anat Rec* 244: 444-451, 1996.

43. **Soffler, Hermanson JW**. Muscular design in the interosseus muscle. *J Morphol* 267: 696-704, 2006.

44. **Sosnicki AA, Lutz GJ, Rome LC, Goble DO.** Histochemical and molecular determination of fiber types in chemically skinned single equine skeletal muscle fibers. *J Histochem Cytochem* 37: 1731-1738, 1989.

45. **Stephenson DG, Williams DA.** Calcium-activated force responses in fast- and slow-twitch skinned muscle fibers of the rat at different temperatures. *J Physiol* 317: 281-302, 1981.

46. **Stienen GJ, Kiers JL, Bottinelli R, Reggiani C.** Myofibrillar ATPase activity in skinned human skeletal muscle fibers: fiber type and temperature dependence. *J Physiol* 493: 299-307, 1996.

47. **Swanstrom MD, Zarucco L, Stover SM, Hubbard M, Hawkins DA, Driessen B, Steffey EP.** Passive and active mechanical properties of superficial and deep digital flexor muscles in the forelimbs of anesthetized Thoroughbred horses. *J Biomech* 38: 579-586, 2005.

48. **Talmadge RJ, Roy RR.** Electrophoretic separation of rat skeletal muscle myosin heavy-chain isoforms. *J Appl Physiol* 75: 2337-2340, 1993.

49. **Toniolo L, Patruno M, Maccatrozzo L, Pellegrino MA, Canepari M, Rossi R, D'Antona GD, Bottinelli R, Reggiani C, Mascarello F**. Fast fibers in a large animal: fiber types, contractile properties and myosin expression in pig skeletal muscles. *J Exp Biol* 207: 1875-1886, 2004.

50. **Toniolo L, Maccatrozzo L, Patruno M, Caliaro F, Mascarello F, Reggiani C.** Expression of eight distinct MHC isoforms in bovine striated muscles: evidence for MHC-2B presence only in extraocular muscles. *J Exp Biol* 208: 4243-4253, 2005.

51. **Wang G, Kawai M.** Effect of temperature on elementary steps of the cross-bridge cycle in rabbit soleus slow twitch muscle fibers. *J Physiol* 531: 219 234, 2001.

52. **Widrick JJ, Trappe SW, Blaser CA, Costill DL, Fitts RH.** Isometric force and maximal shortening velocity of single muscle fibers from elite master runners. *Am J Physiol* 271, **(***Cell Physiol* 40): C666-C675, 1996.

53. **Widrick JJ, Romatowski JG, Karhanek M, Fitts RH.** Contractile properties of rat, rhesus monkey, and human type I muscle fibers. *Am J Physiol* (*Reg Int Comp Physiol*) 272: R34-42, 1997.

54. **Zarucco L, Taylor KT, Stover SM.** Muscle architecture and fiber characteristics of the superficial and deep digital flexor muscles in adult Thoroughbred horses. *Am J Vet Res* 65: 819-828, 2004.

55. **Zhao Y, Kawai M.** Kinetic and thermodynamic studies of the cross-bridge cycle in rabbit psoas muscle fibers. *Biophys J* 67: 1655-1688, 1994.

Acknowledgments

The authors would like to thank the Cornell University, College of Veterinary Medicine, Department of Necropsy for access to horses for muscle tissue biopsies. We thank Lori McFadden and Victor Miller for assistance in preparation and purification of myosin, HMM and actin. We thank Dr. Aya Kataoka Takeda and Janina Bhuvasorakul for assistance with fiber data analyses. We also wish to specially thank Dr. Douglas Syme for resources and assistance with myosin heavy chain SDS-PAGE and analysis of gels. Portions of this work were submitted as a doctoral dissertation at the University of Calgary by MTB. Preparation of this manuscript was permitted by teaching reassignment time at Youngstown State University. The present address for NM Brunet is: Centre for Cognitive Neuroimaging, Donders Institute for Brain, Cognition and Behaviour, Radboud University, Nijemen Netherlands.

Grants

This work was supported in part by NIH HL63974 and NASA/NSBRI MA00211 to PB Chase, and American Heart Association Florida/Puerto Rico Affiliate Pre-Doctoral Fellowship 0315097B to NM Brunet. This work was also supported by an NSERC Grant to D. Syme. Some initial data were generated with support from NSF IBN 9819985 to JH Hermanson and JEA Bertram.

Figure Legends

Figure 1. Representative serial sections from the DDF muscle (humeral head, short compartment). Slow fibers appear darker than fast fibers after myosin ATPase staining following preincubation at pH 4.4 (**A)** or after incubation with anti-slow myosin antibody S58 (**B**). Fast fibers stained darker than slow fibers after reaction against anti-fast myosin antibodies MY32 (**C)** or SC71 (**D**); SC71 recognizes only the MHC-2A isoform. For reference, one fiber has been labeled with an asterisk in all panels. Note that myosin ATPase preincubations were done at pH 4.3, 4.4, 4.5 and 10.3. The scale bar is 100 μm.

Figure 2. Composite of MHC isoform gels (SDS-PAGE) of single, skinned DDF, SDF and SOL muscle fibers. Samples from individual gels are separated by vertical heavy grey lines. On the left are two sample gel lanes run with bulk bundle myosin preparations (illustrated are SOL and DDF) that were used as MHC isoform references (see Methods); the first lane shows the slow MHC-1 isoform from a SOL myosin sample, while the second lane clearly shows both the MHC-1 isoform and a fast MHC-2A isoform from a DDF myosin sample. The latter is representative of bulk myosin from either DDF or SDF bundles, although the proportions of the two MHC bands vary. All other lanes show MHC bands present in example single fibers from DDF (two fibers), SDF (three fibers) or SOL (two fibers). MHC-1 and MHC-2A were the only two

isoforms identified by SDS-PAGE in the population of DDF and SDF fibers sampled from 5 horses. Some hybrid fibers of the MHC-1-2A isoforms (co-expression) were found in the sample and are illustrated by a single SDF fiber (SDF D). Only MHC-1 was found in SOL fibers. Representative examples of two SOL fibers from different horse donors (D, E) are shown on the far right.

Figure 3. V_f (mean ± SE) measured from motility assays for horse DDF, SDF or rabbit psoas muscle HMM. (*****) V_f for DDF and SDF HMM was significantly lower than V_f of rabbit psoas measured at the same temperature (28°C or 38°C). (‡) V_f for SDF HMM was significantly lower than V_f of DDF measured at the same temperature (28°C and 38°C). Number of individual actin filaments analyzed was n = 180 for each temperature and each muscle.

Figure 4. Example chart record of single, skinned DDF fiber force at 30°C, illustrating the time course of the overall experimental protocol. Fibers were initially activated in high Ca^{2+} solution (pCa 5) (left). Following activation, passive tension (pCa 9; relaxing) was minimized and isometric sarcomere length (L_s) and thus final fiber length (L_0) were set. Isometric force (P) was measured over a range of increasing [Ca^{2+}]'s (decreasing pCa's), ending in the highest (P_0 at pCa 5; maximal activation). Measurements of P were taken after force reached steady-state at each Ca^{2+}. Downward arrows indicate changes in gain. After P_0 measurement at pCa 5, fibers were briefly relaxed and then maximal activation at pCa 5 was again induced for slack test determination of velocity of unloaded shortening (V_{US}). Notice the similarity of force during first and last activations, indicating stability of function throughout the protocol.

Figure 5. Frequency distributions for P_0/CSA (A) and V_{US} (B) of SOL (light grey), SDF (black) and DDF (dark grey) fibers at pCa 5 and 30°C. Histogram A does not indicate a bimodal

distribution of P_0/CSA among DDF, SDF and slow (MHC-1) SOL fibers. Note in histogram B the apparent bimodal distribution of V_{US} values from individual DDF fibers.

Figure 6. Force-Ca^{2+} relationships of DDF (A), SDF (B) and SOL (C) fibers at 10°C (open symbols and black dashed lines) and 30°C (filled circles and solid lines). Force (ordinate) is normalized to its value at maximal activation (pCa 5) minus passive tension (pCa 9). Ca^{2+} concentration (pCa) increases from left (pCa 9; relaxing) to right (pCa 5); force increases with decreasing pCa. Each data point represents mean (± SE) of n = 11 DDF fibers, n = 10 SDF fibers, or n = 9 SOL fibers: mean values from each fiber experiment and muscle are shown for clarity. Hill regressions for individual fiber experiments at each temperature showed strong relationships with average $R^2 \geq 0.95$. pCa_{50} (pCa at which P = 50% P_0) at 30°C is given in each panel.

Tables

Table 1. Percentage distributions of MHC fiber type from SDS-PAGE analysis on single, skinned DDF, SDF, and SOL fibers from the five donor horses.

	DDF				SDF				SOL			
Horse	MHC-1 (%)	MHC-2A (%)	MHC-1-2A (%)	*n*	MHC-1 (%)	MHC-2A (%)	MHC-1-2A (%)	*n*	MHC-1 (%)	MHC-2A (%)	MHC-1-2A (%)	*n*
A	--	87.5	12.5	8	50.0	50	--	8				
B	37.5	50.0	12.5	16	46.7	46.7	6.7	15				
C	--	100	--	8	85.7	--	14.3	7				
D	17.4	82.6	--	23	50.0	46.2	3.8	26	100	--	--	26
E	--	100	--	24	21.7	65.2	13.0	23	100	--	--	13
Population (%):												
	12.7	**83.5**	**3.8**		**44.3**	**48.1**	**7.6**		**100**	**0**	**0**	

MHC-1-2A is a hybrid slow, fast fiber type.

Table 2. Means ± SEM of isometric tension (P_0/CSA) and velocity of unloaded shortening (V_{US}) measured at pCa 5 for DDF, SDF and SOL (slow muscle control) fibers.

Muscle	Temperature (°C)	Fiber CSA (μm^2)	P_0/CSA (mN mm^{-2})	V_{US} (FL s^{-1})
DDF	30	6459 ± 512	104 ± 8.8*† (22)	2.4 ± 0.5 (12)
	10		93.3 ± 7.3*† (24)	0.7 ± 0.2* (13)
SDF	30	4615 ± 341	81.8 ± 7.7 (24)	1.2 ± 0.2 (12)
	10		73.1 ± 7.5* (22)	0.6 ± 0.2* (11)
SOL	30	1775 ± 102	78.1 ± 6.0 (11)	1.1 ± 0.2 (9)
	10		46.7 ± 4.5 (11)	0.3 ± 0.1 (9)

Values are means ± SE
In parentheses are the number (*n*) of fibers analyzed
* Significantly different from SOL at $p < 0.05$ for corresponding temperature
† Significantly different from SDF at $p < 0.05$ for corresponding temperature

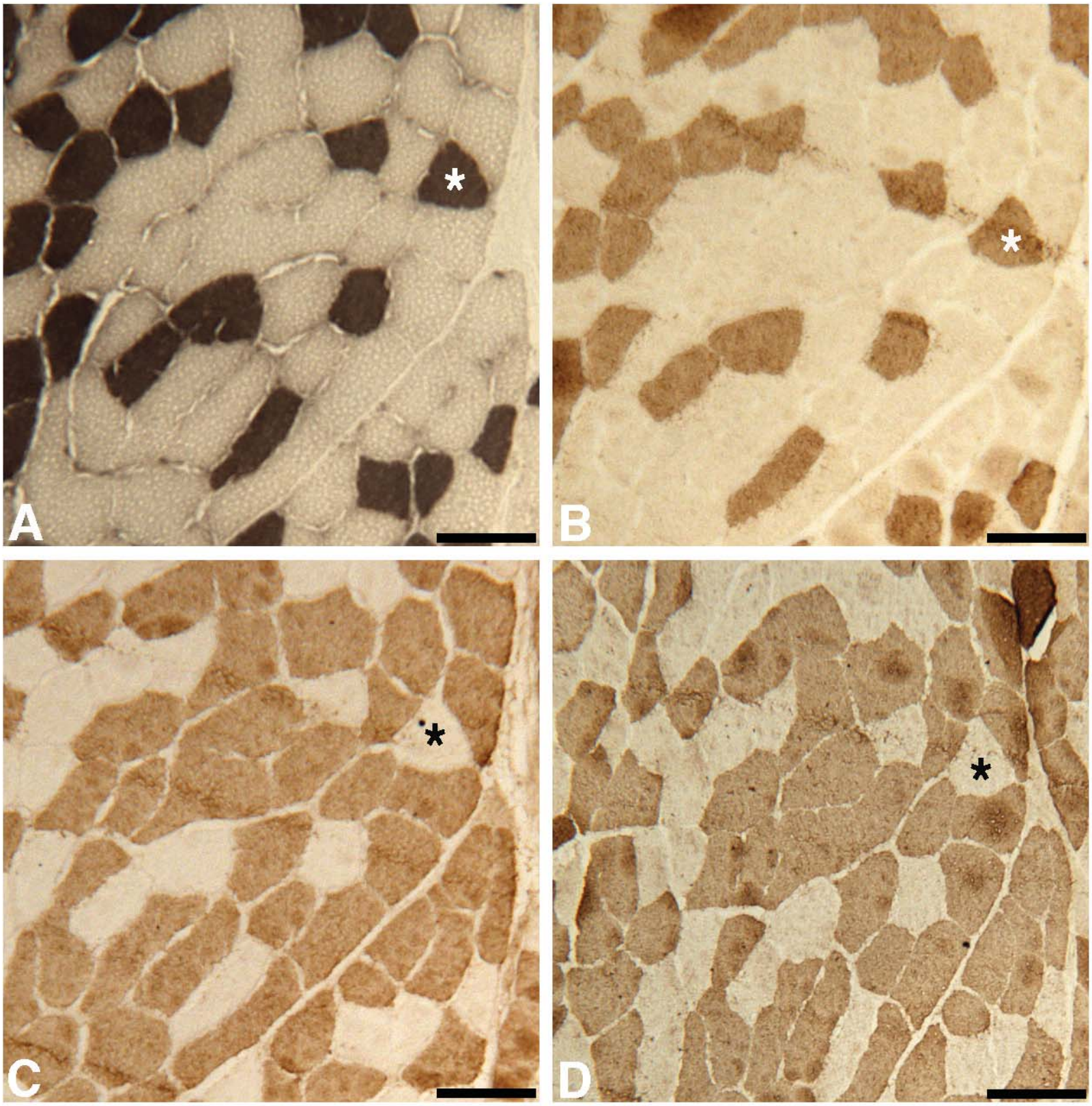
A
B
C
D

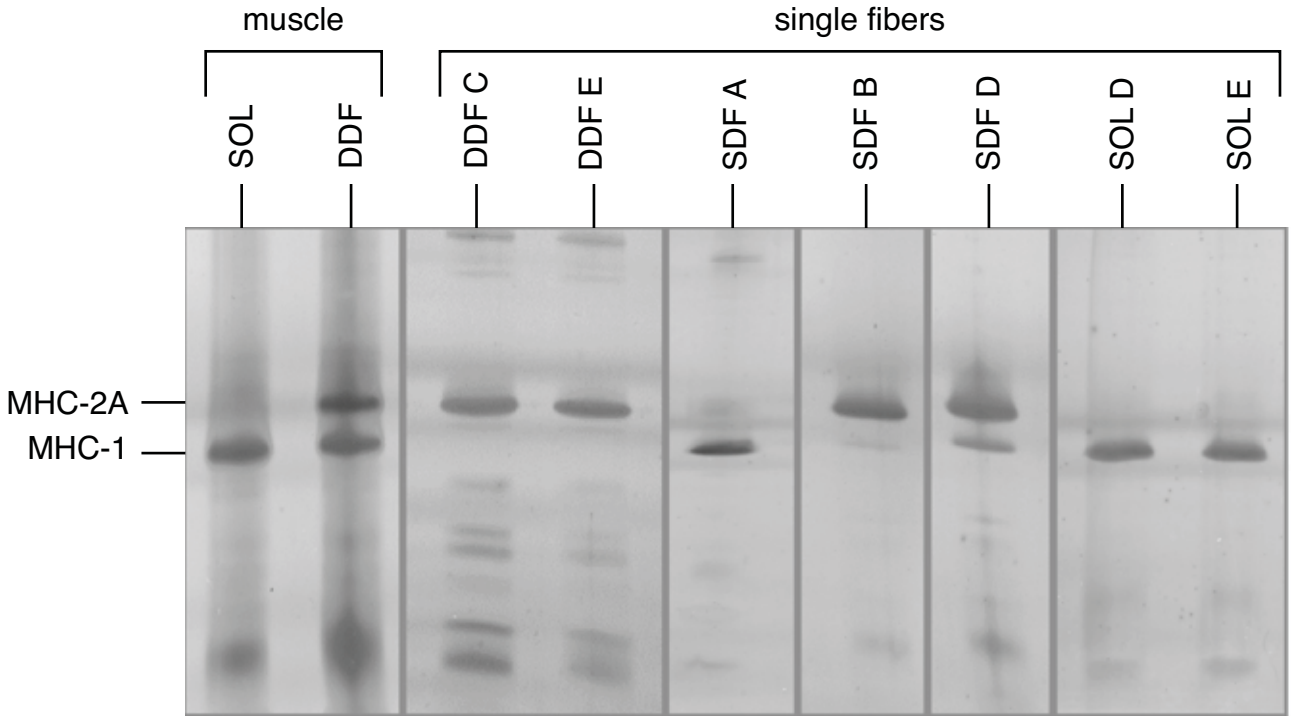
muscle
single fibers
SOL
DDF
DDF C
DDF E
SDF A
SDF B
SDF D
SOL D
SOL E
MHC-2A
MHC-1

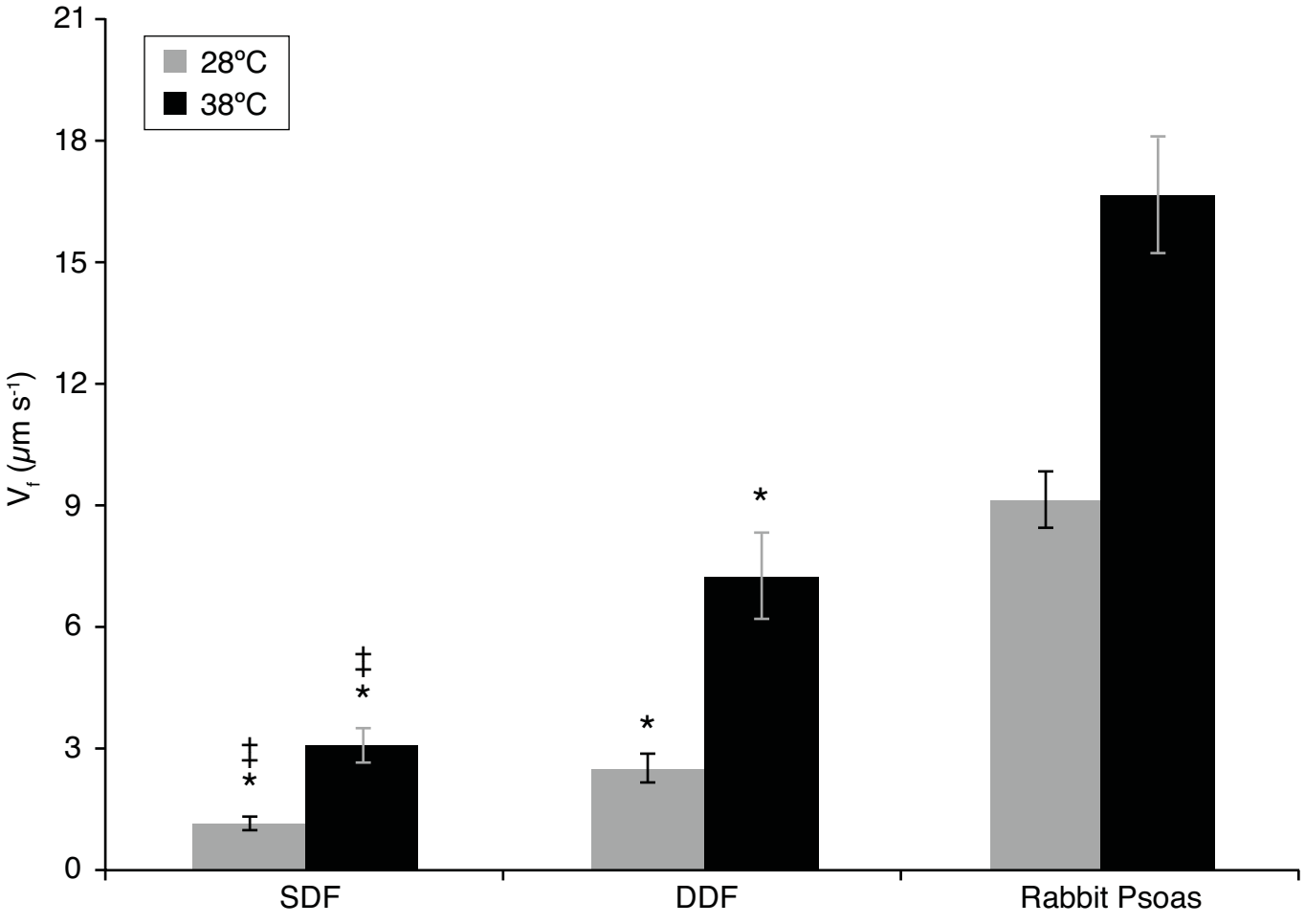
21
18
15
12
9
6
3
0
28°C
38°C
V_f (μm s^{-1})
‡
*
‡
*
*
*
SDF
DDF
Rabbit Psoas

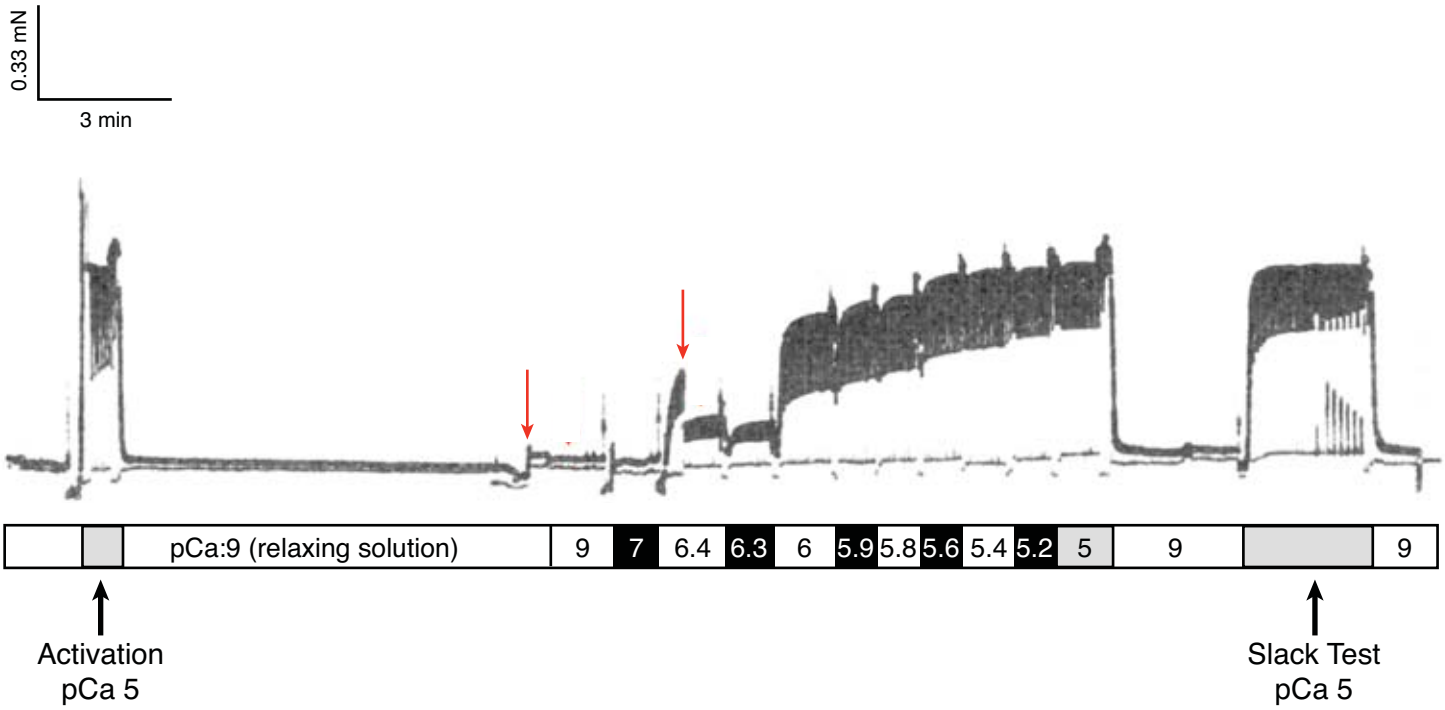
0.33 mN
3 min
pCa:9 (relaxing solution)
9
7
6.4
6.3
6
5.9
5.8
5.6
5.4
5.2
5
9
9
Activation
pCa 5
Slack Test
pCa 5

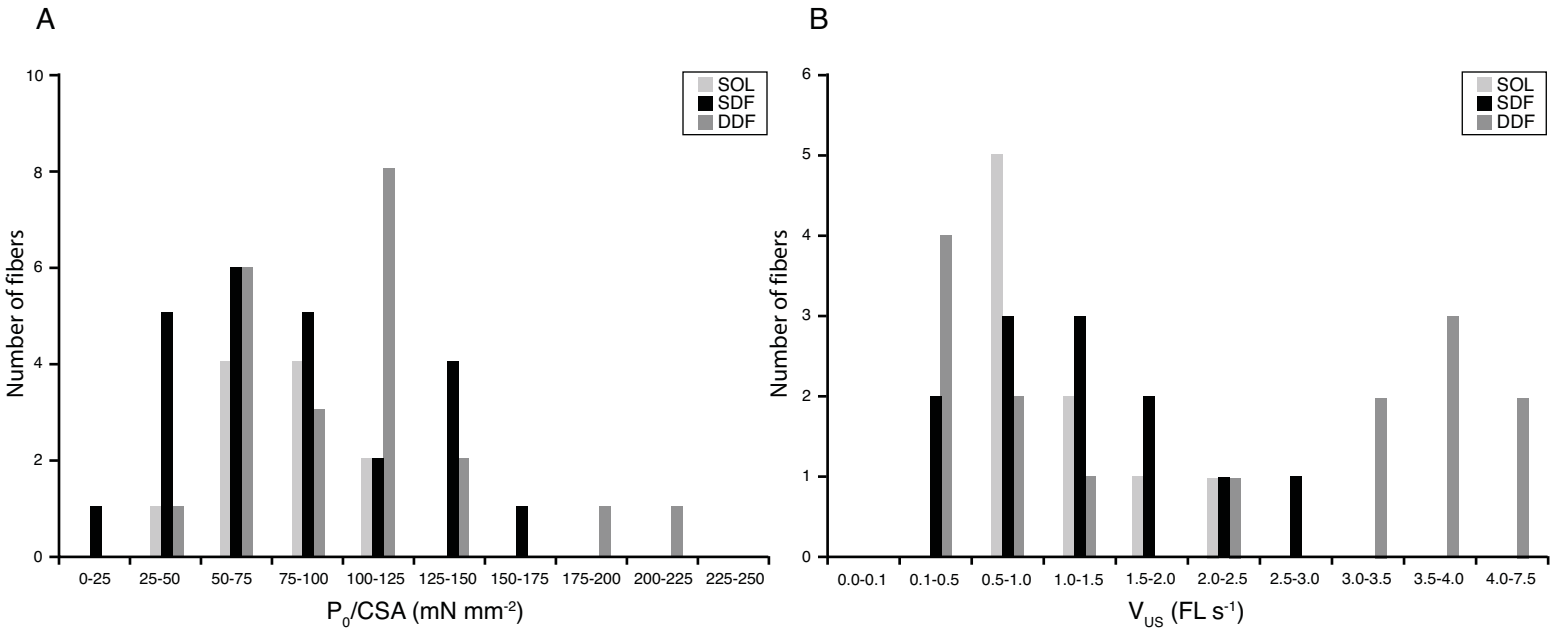
A
B
SOL
SDF
DDF
Number of fibers
0
2
4
6
8
10
0-25
25-50
50-75
75-100
100-125
125-150
150-175
175-200
200-225
225-250
P0/CSA (mN mm-2)
1
3
5
0.0-0.1
0.1-0.5
0.5-1.0
1.0-1.5
1.5-2.0
2.0-2.5
2.5-3.0
3.0-3.5
3.5-4.0
4.0-7.5
VUS (FL s-1)

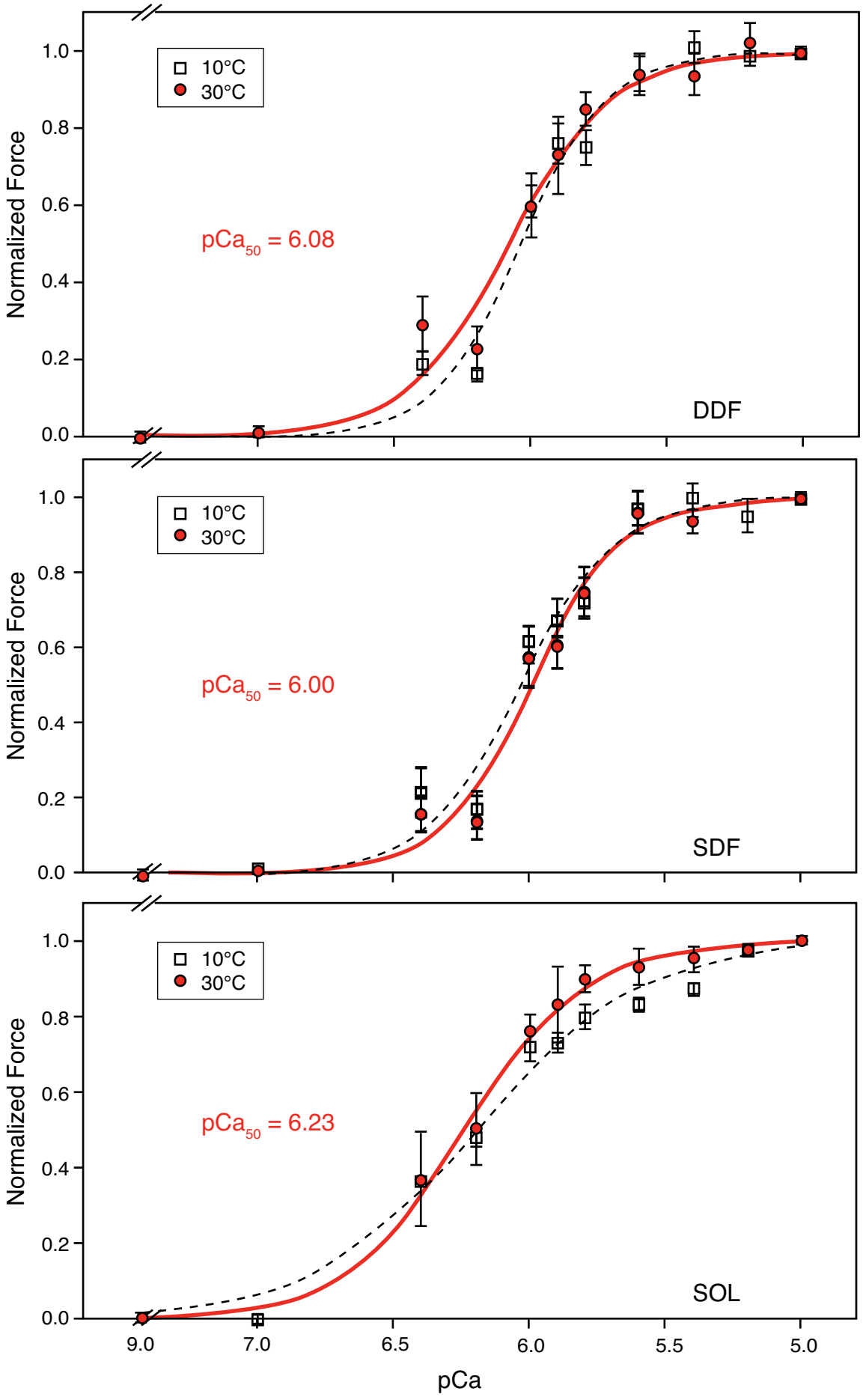
10°C
30°C
pCa50 = 6.08
DDF
10°C
30°C
pCa50 = 6.00
SDF
10°C
30°C
pCa50 = 6.23
SOL
Normalized Force
1.0
0.8
0.6
0.4
0.2
0.0
9.0
7.0
6.5
6.0
5.5
5.0
pCa